TRANSMEMBRANE ELECTRICAL CURRENTS OF SPIN-LABELED HYDROPHOBIC IONS

DAVID S. CAFISO
Department of Chemistry, University of Virginia, Charlottesville, Virginia 22901

WAYNE L. HUBBELL
Department of Chemistry, University of California, Berkeley, California 94720

ABSTRACT When spin-labeled phosphonium ions are rapidly mixed with phospholipid vesicles, time-dependent changes in the electron paramagnetic resonance spectrum of the spin label are observed. These changes are interpreted in terms of transmembrane transport of the hydrophobic ion, and simple analysis of the data at different membrane potentials is shown to give the binding constant of the ion to both membrane surfaces, the permeability, and current-voltage relationship for the vesicle membrane in the presence of the hydrophobic ion. These results establish the time resolution for methods using the phosphonium ion as a probe of time-dependent potentials across vesicle membranes, as well as provide fundamental information regarding the binding and transport of hydrophobic cations across bilayers. This latter point is significant in view of the fact that hydrophobic cations have not been well characterized in planar bilayers due to their weak binding and low conductance.

INTRODUCTION

Electrical properties of biological membranes are traditionally investigated by the use of intracellular microelectrode methods and more recently by patch-clamp techniques. These approaches can give extremely detailed, highly time-resolved information on bulk electrical properties and their modulation, but its application is restricted to cells or organelles of sufficiently large size. At present, many membrane systems of great interest are too small to be amenable to the powerful microelectrode methods. Even for systems that can be studied by microelectrodes, a final molecular understanding will most likely be preceded by isolation and reconstitution procedures which yield small membrane vesicles ideal for chemistry but impenetrable by microelectrodes. In addition, the use of electrode methods gives direct information only on bulk phase potential differences; it would be extremely desirable to obtain information pertaining to microscopic electrical properties for membrane systems.

New methods for investigating electrical properties are thus under active investigation, and approaches based on hydrophobic ions (Bakeeva et al., 1970; Shuldiner and Kaback, 1975; Grollman et al., 1977; Andersen, 1978; Kamo et al., 1979; Macey and Orme, 1980), organic dyes (see Waggoner, 1979, for a review), electrochromic effects on carotenoids (Emrich et al., 1969 *a*, *b*), and spin labels (see Cafiso and Hubbell, 1981, for a review) have been reported. In earlier work, it has been shown that information on equilibrium distributions of hydrophobic spin labels, such as the phosphonium ion shown below, that we refer to as (I),

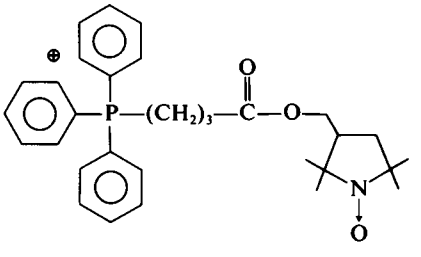

can give values of transmembrane electric potential in phospholipid vesicles (Cafiso and Hubbell, 1978). As an extension of this method, we are now investigating the application of spin-labeled hydrophobic ions such as (I) to non-equilibrium electrical states of phospholipid vesicles in an attempt to estimate time-dependent transmembrane potentials and hence ionic currents. The time resolution with which one can observe potential transients by this method depends on the permeability of spin-label phosphonium ions in the membrane system of interest. In the present paper, we present results of a study of the flow of spin label (I) across sonicated phosphatidylcholine vesicles and show that a simple analysis yields the membrane conductance, the membrane permeability, and the current-voltage characteristics of the membrane in the presence of phosphonium (I). These results demonstrate the utility of the method in investigating time-dependent electrical phenomena and lay the foundation for the use of the phosphonium ion to estimate transmembrane currents of other ions.

EXPERIMENTAL

Synthesis of (I) and Purification of Phosphatidylcholine

The synthesis of the spin-labeled phosphonium (I) was accomplished as described previously (Cafiso and Hubbell, 1978).

Egg phosphatidylcholine (PC) was prepared according to the procedure of Singleton et al. (1965) and stored at −20°C in $CHCl_3$ under an argon atmosphere.

Phospholipid Vesicles and Generation of Transmembrane Potentials

To prepare vesicles, the chloroform from an aliquot of PC was removed by a stream of argon and the lipid was then dried by vacuum desiccation for a minimum of 15 h. The dispersion of this lipid in the appropriate buffer solution and subsequent sonication were carried out as described previously (Cafiso and Hubbell, 1978). The vesicles were found by negative stain and platinum shadowing techniques (Castle and Hubbell, 1976) to have a diameter of ~300 Å.

Final concentrations of phospholipids in sonicated suspensions were determined by phosphate analysis, essentially according to Bartlett (1959).

In the analyses discussed in this paper, we repeatedly use certain geometrical features of the vesicle population: S_o, V_o/V_i and V_{mo}/V_{mi}. S_o is the total external surface area of the vesicles per liter of suspension and is computed as $S_o = 3.8 \times 10^6 \cdot m$ where m is the mass (in grams) of lipid per liter of suspension, and S_o is in cm^2 per liter. This equation assumes an average of 70 $Å^2$ per phospholipid in the membrane, an average molecular weight for egg PC of 770 and vesicle inner and outer radii of 100 and 150 Å, respectively (Castle and Hubbell, 1976). V_o/V_i is the ratio of external aqueous volume to the internal aqueous volume and is determined as described previously from phosphate analysis of the vesicle suspension (Cafiso and Hubbell, 1978). Typically, V_o/V_i ranged from 40–50 in these experiments. V_{mo}/V_{mi} is the ratio of volumes of the external and internal binding regions of the vesicle and was estimated, as previously described, to be ~2.3 for vesicles with an external radius of 150 Å (Cafiso and Hubbell, 1978).

Transmembrane potentials were created by the addition of valinomycin (final concentration 10^{-5} M) to vesicle suspensions across which the desired K^+ gradient had been established. Unless otherwise noted, vesicle suspensions contained 50 mM morpholinopropane sulfonic acid (MOPS) buffer, pH = 7.0, and Na_2SO_4 and/or K_2SO_4 such that $[K_2SO_4] + [Na_2SO_4] = 0.225$ M. Potassium gradients were established by salt exchange on a column of BioGel A 0.5 M (Bio-Rad Laboratories, Richmond, CA) as described earlier (Cafiso and Hubbell, 1978). Upon the addition of valinomycin to sonicated egg PC vesicles, the K^+ equilibrium potentials thus created decreased by only ~10% over an 8 h period at room temperature (Cafiso and Hubbell, 1978).

In some experiments, it was necessary to mix the phosphonium and phospholipid vesicles rapidly. To accomplish this, solutions of (I) and vesicles were contained in separate syringes which could be simultaneously driven by a pneumatic plunger system (Science Products Corporation). The effluents from the syringes were mixed in a low-volume teflon chamber immediately before entering a sample cell contained in the microwave cavity. Complete mixing and delivery to the sample cell could be achieved within ~40 ms.

Treatment of Data and Determination of Initial Rates

In the experiments presented below, EPR spectral amplitudes $[A_f - A_f(\infty)]$ are obtained as a function of time. These data are fitted to an exponential function of the form of Eq. 6 in the text using a least-squares analysis. From the analysis, values of the exponential decay constant (γ) and the relaxation amplitude $[A_f(0) - A_f(\infty)]$ are obtained. The initial rate of change in the signal amplitude is calculated as $(dA_f/dt)_{t=0} = -\gamma[A_f(0) - A_f(\infty)]$.

ANALYSIS OF EPR SPECTRA

As shown previously (Cafiso and Hubbell, 1978; 1981), the decrease in the high-field resonance amplitude (A) of the electron paramagnetic resonance (EPR) spectrum of (I) in the presence of vesicles is due to the equilibrium binding of (I) to the membrane surfaces. In the presence of membranes, the amplitude A is thus the sum of contributions from free and bound populations of (I). In the present experiments, we desire the amplitude due to the free population alone, A_f. The analysis of such spectra has been discussed previously (Cafiso and Hubbell, 1978; 1981) and the result pertinent for the present discussion is

$$A_f = \frac{A - \beta/\alpha A_f^\circ}{1 - \beta/\alpha} \tag{1}$$

where A_f° is the amplitude of the high-field resonance line in the absence of membranes and the constants α and β are defined by

$$N_b = \alpha A_b \tag{2}$$

$$N_f = \beta A_f \tag{3}$$

where A_b, A_f are the resonance amplitudes corresponding to N_b and N_f moles of bound and free spins, respectively, in a liter of vesicle suspension. To determine A_f from experimental values of A, the constant β/α must be known. This value is readily determined by recording EPR spectral amplitudes of equal moles of (I) completely bound to vesicles (A_b°) and completely free in the absence of vesicles (A_f°). Because the number of moles is the same in each sample, we have from Eq. 2, $A_b^\circ/A_f^\circ = (\beta/\alpha)$. The sample with (I) completely bound was prepared by using a high vesicle concentration (~5% wt/vol lipid) and high inside-negative transmembrane potential. The value of β/α for (I) in PC membranes was found in this way to be −0.033. Experimental data of A vs. time can thus be transformed to A_f vs. time by use of Eq. 1.

Fig. 1 *a* shows a recording of A vs. time after rapid mixing of phospholipid vesicles with an equal volume of a 4×10^{-5} M solution of (I). The decrease of A in time after mixing corresponds to an increase in the amount of (I) bound to the membrane. The increased binding is interpreted to be due to the transmembrane migration of (I) after the rapid mix. This result is expected because the amount of membrane binding surface increases as the label migrates to the interior volume of the vesicle. Before presenting further data, we first discuss a simple model that we will use to analyze this type of data.

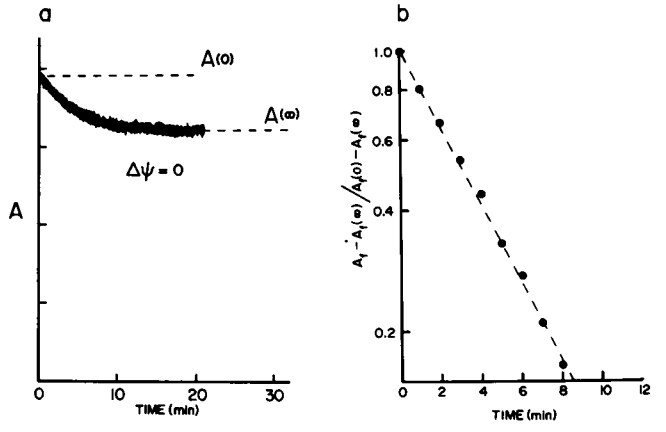

FIGURE 1 (*a*) Recording (retraced) of A after rapid mixing of a phospholipid vesicle suspension with an equal volume of a 4×10^{-5} M solution of (I). $A(0)$ represents the initial and $A(\infty)$ the equilibrium amplitude for the relaxation. In this sample, egg PC was at a concentration of 35.6 mg/ml, with $K^+_{in}/K^+_{out} = 1$ in the presence of 10 μM valinomycin. (*b*) The fractional change in the free signal amplitude for the preceeding data is plotted on a log scale vs. time.

A MODEL FOR THE TRANSPORT OF (I) ACROSS THE BILAYER OF PHOSPHOLIPID VESICLES

It is now generally accepted that the potential energy profile of a hydrophobic ion across a bilayer is of the general form shown in the upper part of Fig. 2. The central barrier arises from a position-dependent electrostatic charging energy, while the potential energy minima near the interfaces are characteristic of hydrophobic ions and have major contributions from the favorable free energy of transfer of the hydrophobic groups from water to the membrane interior. These minima represent the binding regions of hydrophobic ions to membrane interfaces. For a detailed discussion of the shape and origin of such energy profiles, the interested reader should consult the original papers in this area (Neumke and Laüger, 1969; Ketterer et al., 1971; Andersen and Fuchs, 1975). It should be pointed out that the potential energy profile in Fig. 2 is purely schematic, and for a phosphonium ion the depth and displacement from the surface of the potential energy minima are greatly exaggerated, as will be discussed below. In this paper four discrete regions of space occupied by the phosphonium in the vesicle system are identified (see Fig. 2): the external aqueous solution (o), the external membrane binding site (mo), the internal membrane binding site (mi), and the internal aqueous solution (i). The volumes of the regions per liter of vesicle suspension are V_o, V_{mo}, V_{mi}, and V_i, respectively. The numbers of moles of (I) residing in each region per liter of vesicle suspension are N_o, N_{mo}, N_{mi}, and N_i, respectively, and the concentrations of spin label (I) in each region are $[I]_o$, $[I]_{mo}$, $[I]_{mi}$, and $[I]_i$.

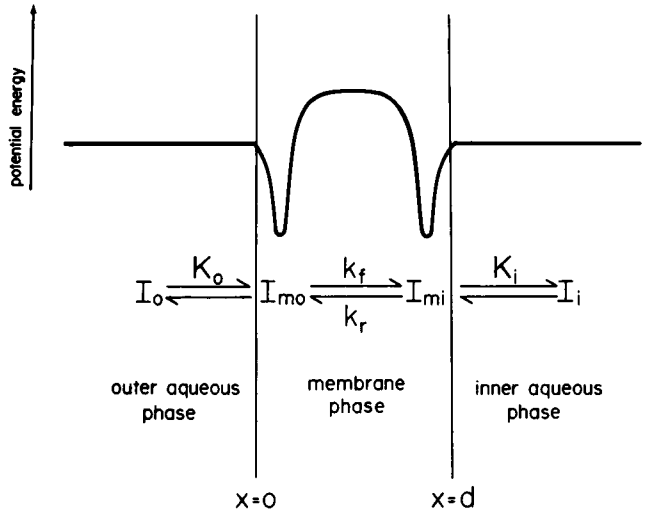

FIGURE 2 Potential energy profile and three-step transport mechanism for hydrophobic ions across a thin hydrocarbon membrane (according to Ketterer et al., 1971). I_o, I_{mo}, I_{mi}, and I_i represent spin label (I) in the regions o, mo, mi, and i, respectively. The regions o and i are the exterior and interior aqueous phases, mo and mi are the external and internal regions representing the potential energy minima where the hydrophobic ions bind. The position and depth of the potential energy minima are schematic and the profile is not a scaled representation for the phosphonium ion spin label.

The flow of hydrophobic ions across membranes is satisfactorily described by the three-step mechanism proposed by Ketterer et al. (1971) (see Fig. 2). The ion first adsorbs to one membrane surface at the position of the potential energy minimum, then crosses the membrane interior in an elementary step and finally desorbs from the opposite membrane surface. For hydrophobic cations, the transmembrane step (with rate constants k_f and k_r) appears to be rate limiting (Pickar and Benz, 1978) and we assume here that the interfacial binding processes are at all times at equilibrium with equilibrium constants K_o and K_i for the outer and inner surface, respectively. The results discussed below provide support for this kinetic model of the flow of (I) across the membranes of phospholipid vesicles.

When (I) is rapidly mixed with a membrane vesicle sample, equilibrium binding with the external surface is reached within the mixing time ($\approx$ 40 ms), and the initial amplitude, $A_f(0)$, then represents the amount of free (I) in equilibrium with the external surface at time zero. $A_f(0)$ is related to the binding constant at the external surface by

$$\frac{A_f^\circ}{A_f(0)} - 1 = K_o \frac{V_{mo}}{V_o}. \tag{4}$$

Because the binding region is very close to the surface of the membrane, the binding constants are expected to be independent of transmembrane potential, and data presented elsewhere (Cafiso and Hubbell, 1978) and below support this conclusion. The final amplitude, $A_f(\infty)$, repre-

sents equilibrium binding of (I) to both membrane surfaces, and it has been previously demonstrated that the potential dependence of $A_f(\infty)$ can be accounted for by

$$\frac{A_f^\circ}{A_f(\infty)} - 1 = \frac{K_i \frac{V_{mi}}{V_i} + K_o \frac{V_{mi}}{V_{mo}} e^{\phi}}{1 + \frac{V_o}{V_i} e^{\phi}} \tag{5}$$

where ϕ is the reduced potential, $\phi = \Delta\psi ZF/RT$, and $\Delta\psi$ is the transmembrane potential (Cafiso and Hubbell, 1978). If the transmembrane movement of (I) during the approach to equilibrium is viewed as a single elementary step, the time dependence of A_f (Appendix A) is given by

$$[A_f - A_f(\infty)] = [A_f(0) - A_f(\infty)]e^{-\gamma t} \tag{6}$$

where γ is the rate constant for relaxation to equilibrium and is defined as

$$\gamma = k_f + k_r \frac{K_i}{K_o} \frac{V_{mi}}{V_{mo}} \frac{V_o}{V_i} \frac{\epsilon_o}{\epsilon_i}. \tag{7}$$

In Eq. 7, k_f and k_r are the rate constants identified in Fig. 2, and $\epsilon_o = 1 + K_o V_{mo}/V_o$; $\epsilon_i = 1 + K_i V_{mi}/V_i$.

In the presence of a transmembrane potential, the rate constants k_f and k_r will be modified, and the voltage dependence of the rate constants can be found either from a Nernst-Planck (Benz et al., 1976) or Eyring rate analysis (Ketterer et al., 1971). The former requires detailed knowledge of the potential energy profiles of (I) throughout the membrane. Although reasonable potential-energy profiles are available (Neumcke and Laüger, 1969; Hall et al., 1973; Andersen and Fuchs, 1975; Ginsburg and Noble, 1976) we have used the simpler Eyring approach for a single barrier because it accounts fairly well for the data. If it is assumed that there is one well-defined energy barrier to ion flow located within the membrane, then

$$k_f = k_f^\circ e^{-n\phi} \tag{8}$$

$$k_r = k_r^\circ e^{(1-n)\phi}, \tag{9}$$

where k_f° and k_r° are the transport rate constants in the absence of a transmembrane potential and n is the fraction of the transmembrane potential that drops from the outer membrane surface to the barrier peak (Ginsburg and Noble, 1976). For a constant field and symmetric membrane (such as planar bilayers), one expects $n = 0.5$ for a sharp central barrier. For small sonicated spherical vesicles, however, one cannot assume a constant field, nor can one necessarily assume a centrally located barrier. Eqs. 8 and 9 with values of n other than 0.5 can also be used to mathematically represent barrier shapes other than sharply peaked central barriers (Ginsburg and Noble, 1976). The quantity n will thus be treated as a parameter in analyzing the rate data.

Including this voltage dependence of the rate constants explicitly, Eq. 7 can be written as (see Appendix A)

$$\gamma = k_f^\circ \left[e^{-n\phi} + \frac{\epsilon_o}{\epsilon_i} \frac{V_o}{V_i} e^{(1-n)\phi} \right]. \tag{10}$$

The transmembrane current density of (I) at the outer membrane surface is

$$i = ZF P \{[I]_o e^{-n\phi} - [I]_i e^{(1-n)\phi}\} \tag{11}$$

where P is the permeability of the membrane to the phosphonium ion and, in terms of parameters of the model (see Appendix B)

$$P \equiv K_o \frac{V_{mo}}{S_o} k_f^\circ. \tag{12}$$

From Eq. 11, it can be seen that the initial current density, i_o, immediately after mixing vesicles with (I) is

$$i_o = ZF P [I]_o e^{-n\phi} \tag{13}$$

Finally, the ohmic membrane conductance is

$$\begin{aligned} \lambda_o &= -\frac{ZF}{RT}\left(\frac{\partial i}{\partial \phi}\right)_{\phi=0} \\ &= \frac{Z^2F^2}{RT} P\{n[I]_o + (1-n)[I]_i\}. \end{aligned} \tag{14}$$

RESULTS

Relaxation in the Absence of Transmembrane Potential

Fig. 1 *a* shows $A(t)$ following a rapid mix of (I) with vesicles in the absence of a transmembrane potential. From this data, $A_f(0)$ and $A_f(\infty)$ are directly obtained through Eq. 1. With these values and Eqs. 4 and 5 at $\phi = 0$, $K_o V_{mo}/V_o$ and $K_i V_{mi}/V_i$ can be estimated from the known value of V_o/V_i (see Methods). Because $K_o V_{mo}/V_o$ depends on vesicle concentration through the volume ratio, it is more convenient to express this binding function by the derived function $K_o V_{mi}/V_i$ which is an intensive property of the vesicle system readily calculated according to

$$K_o \frac{V_{mi}}{V_i} = K_o \frac{V_{mo}}{V_o} \times \frac{V_{mi}}{V_{mo}} \times \frac{V_o}{V_i}.$$

Along with the internal binding function, this function may be used to estimate the ratio of internal-to-external binding constants,

$$\frac{K_i}{K_o} = \frac{K_i V_{mi}/V_i}{K_o V_{mi}/V_i}.$$

For sonicated egg PC vesicles we find from five experiments (±SD) that $K_o V_{mi}/V_i = 15.7 \pm 0.8$, $K_i V_{mi}/V_i = 19.0 \pm 1.0$, and $K_i/K_o = 1.2 \pm 0.1$. Not much significance

should be attached to the relatively small difference in internal and external binding constants calculated in this manner, because a difference of this magnitude could be due to a systematic error introduced through the calculated quantity V_{mi}/V_{mo}.

For the simple transport mechanism considered in Fig. 2, the relaxation to equilibrium should be purely exponential as described by Eq. 6, and the semilogarithmic plot of the $\phi = 0$ data shown in Fig. 1 *b* clearly illustrates that this is the case.

If the observed relaxation of the type shown in Fig. 1 *a* is a simple passive diffusion of (I) across the vesicle as is assumed, the initial current density, i_o, should be proportional to the initial concentration of (I) in the external solution (see Eq. 13). That this expectation is met over the range 10–60 μM of $[I]_o$ is shown in Fig. 3, where the initial rate of change of A_f is taken to be proportional to i_o (see Appendix C). Thus the $\phi = 0$ relaxation phenomena can be quantitatively described in terms of the simple model presented in Fig. 2.

Relaxation in the Presence of a Transmembrane Potential

Fig. 4 shows A as a function of time after rapid mixing of (I) with vesicles having various values of $\Delta\psi$ established with K^+ gradients in the presence of valinomycin. Obvious effects of the transmembrane potential are on the initial rate of change of A and on the final equilibrium value, $A(\infty)$. The quantity $[A_f - A_f(\infty)]$ calculated from each of these curves is accurately represented as a function of time

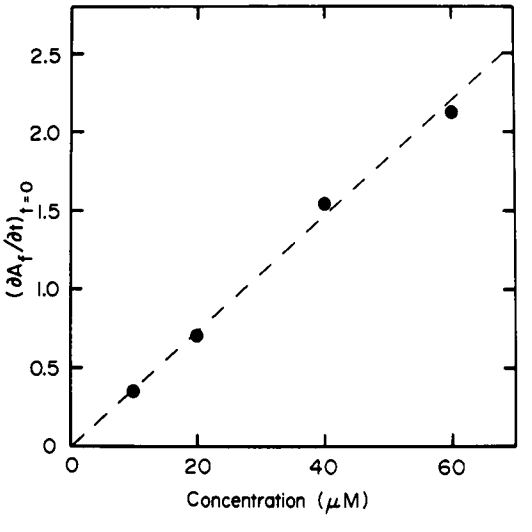

FIGURE 3 A plot of data for (dA_f/dt) at $t = 0$ as a function of the concentration of spin label (I). (dA_f/dt) is the rate of change in the amplitude of the free signal component of (I) and is proportional to the current across the vesicle system, see Appendix C. $(dA_f/dt)_{t=0}$ is plotted in chart units per min where 1.5 chart units corresponds to 1 μM spin label (I). Vesicles are at a PC concentration of 39.4 mg/ml.

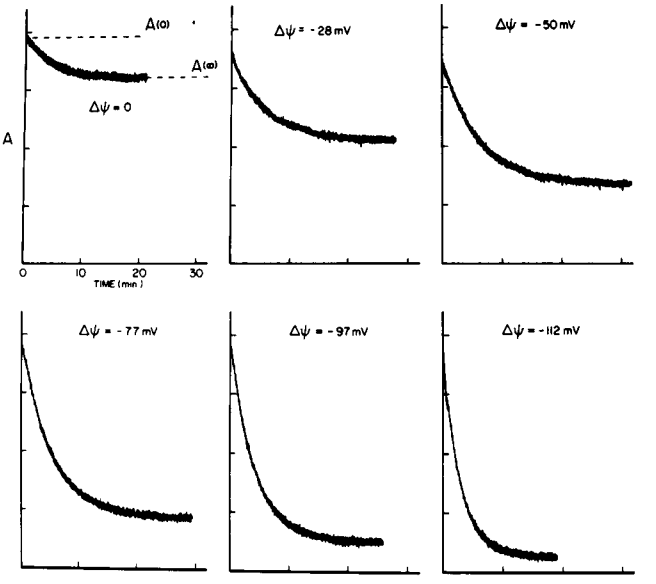

FIGURE 4 Recordings (retraced) of the amplitude of the $m_I = -1$ resonance of spin label (I) vs. time following rapid mixing of (I) (to a final concentration of 20 μM) with vesicles having different values of $\Delta\psi$. The amplitude axis is calibrated by the fact that 20 μM (I) corresponds to 6.6 of the amplitude units on the graph. $\Delta\psi$ is calculated from the K^+ gradient and buffer concentration as described previously by Cafiso and Hubbell (1978) and is in agreement (to within 4 mV) with the experimentally determined values of $\Delta\psi$ obtained from the equilibrium phosphonium distribution. The concentration of vesicles for each case was as follows: $\Delta\psi = 0$, 35.6 mg PC/ml; $\Delta\psi = -28$ mV, 44.2 mg PC/ml; $\Delta\psi = -50$ mV, 46.4 mg PC/ml; $\Delta\psi = -77$ mV, 35.9 mg PC/ml; $\Delta\psi = -97$ mV, 38.1 mg PC/ml; $\Delta\psi = -112$, 46.4 mg PC/ml.

by Eq. 6, and the linearity of the $\ln[A_f - A_f(\infty)]$ vs. time plots are as good as or better than that shown in Fig. 1 *b* for the zero potential relaxation. A least-squares fit of the data in each case gives a coefficient of determination (R^2) of 0.999 or better.

The membrane current density, i, is related (Appendix C) to A_f by

$$i = -\frac{ZF}{S_o}\beta\left(\frac{K_o V_{mo}/V_o}{1 - \epsilon_o/\epsilon_i}\right)\left(\frac{dA_f}{dt}\right). \qquad (15)$$

Thus the first derivatives of the A_f vs. time curves can be used to obtain the membrane current density at any time. In Fig. 5, the initial current density i_o, obtained from $[(dA_f/dt)_{t=0}]$ is plotted vs. the transmembrane electric potential established across the vesicle. This curve illustrates that extremely small current densities are being measured here, on the order of a few pA/cm^2. This relatively high sensitivity is possible because of the enormous surface area of a vesicle suspension and relatively high sensitivity of detection of nitroxyl radicals. The form of the current-voltage curve presented here does not begin at zero current for zero $\Delta\psi$ because a concentration gradient of the phosphonium is present even in the absence of a potential at time zero. From Eq. 13 (at $\phi = 0$) and the

zero voltage initial current from Fig. 5, the forward permeability is established to be 3.8×10^{-9} cm/s. The forward rate constant, k_f^o, may be found directly from the initial slope of the A_f relaxation at $\Delta\psi = 0$ (see Appendix C) and is $7.4 \times 10^{-4}\ s^{-1}$.

An important feature of the current-voltage curve is that it is nonlinear. According to the model discussed above, the initial current-voltage relationship is given by Eq. 13, which predicts an exponential dependence of i_0 on transmembrane voltage. The solid curve in Fig. 5 is drawn according to Eq. 13 with $n = 0.41$ as the only adjustable parameter and the independently determined value of P given above. The agreement is quite satisfactory. The significance of $n = 0.41$ will be discussed in more detail below, but for the present we will investigate more closely the adequacy of the model in accounting for the current flow. So far we have only considered unidirectional flow of charge and its dependence on voltage. According to Eq. 10, however, γ, the rate constant for relaxation to equilibrium, should also be a function of transmembrane potential, although a less sensitive function than the unidirectional rate constant because the forward and reverse rate constants are affected in opposite directions by an applied voltage. Thus the voltage dependence of γ should provide another important test of the mechanism that reflects the voltage dependence of both the forward and reverse rate constants. That γ is indeed voltage dependent is shown by the data in Fig. 6. The points are the values of γ for the relaxations shown in Fig. 4 while the solid line is calculated according to Eq. 10 with $k_f^o = 7.4 \times 10^{-4}\ s^{-1}$ and $n = 0.41$,

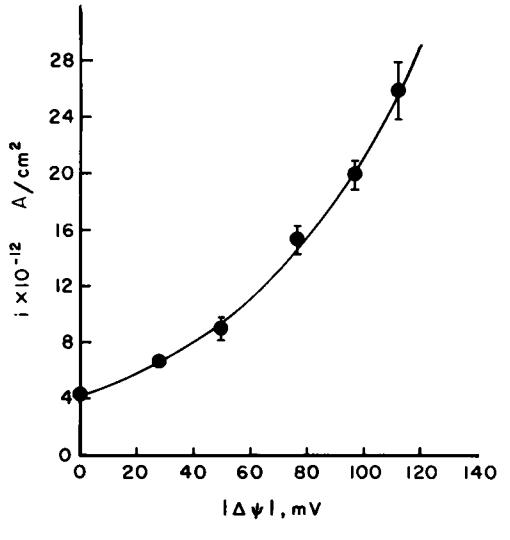

FIGURE 5 Current-voltage curve for spin label (I) in egg-PC vesicles. The data points represent the initial current, i_0, calculated from the initial rates of (dA_f/dt) in Fig. 4 (see Appendix C) and are plotted vs. the transmembrane electric potential across the vesicles. The solid line represents the least-squares fit to the data using Eq. 14 ($R^2 = 0.995$). In this case, the fit gives $n = 0.41$. The error bars are estimated on the basis of a combined random uncertainty of ~10% in the external binding constant and spin label concentration.

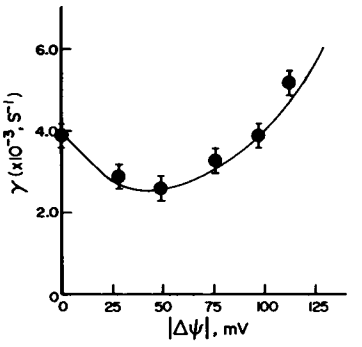

FIGURE 6 A plot of γ, the rate constant for approach to equilibrium vs. transmembrane potential. The points represent values of γ obtained from the relaxations shown in Fig. 4 and the error bars are the estimated uncertainties in the slope (γ) of the least-squares fit to the $\ln[A_f - A_f(\infty)]$ vs. time plot. The solid line is a smooth curve drawn through the calculated points for the various potentials according to Eq. 10 with $k_f^o = 7.4 \times 10^{-4}$ and $n = 0.41$.

the same value found for the voltage dependence of the forward rate constant. Again, the agreement is quite satisfactory, and there are no adjustable parameters.

Effect of Tetraphenylboron (TPB) on the Relaxation Kinetics

The hydrophobic anion tetraphenylboron (TPB) is believed to act as a carrier for certain hydrophobic cations across planar bilayers (Stark, 1980). To see whether TPB acts as a carrier for (I) in the sonicated vesicle system, the relaxation of (I) in the presence of vesicles at $\phi = 0$ was investigated at various levels of TPB. Fig. 7 shows that very low concentrations of TPB (1–5 μM) greatly enhance the

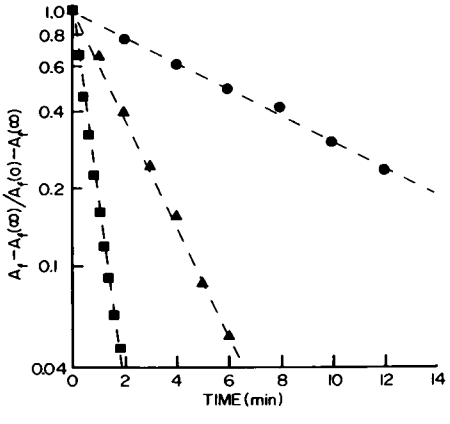

FIGURE 7 Fractional change in the free signal amplitude for 20 μM spin label (I) plotted on a log scale vs. time following rapid mixing of (I) with egg PC vesicles. (●) no added TPB^-, (▲) 1 μM TPB^-, and (■) 5 μM TPB^-. Vesicles are at a concentration of ~40 mg PC/ml and are sonicated in 250 mM MOPS, pH = 6.8. The rate of transmembrane movement in the absence of TPB^- shown here is slower than that shown in Fig. 1. This is due to the presence of valinomycin in the samples from which the data in Fig. 1 were obtained.

permeability of the phosphonium. 5 μM increases the rate constant for approach to equilibrium, γ, by a factor of 14. The approach to equilibrium is still purely exponential as shown by the linearity of the semilogarithmic plots.

The very low levels of TPB (~0.5 TPB molecules per vesicle, maximum) and the high ionic strength of the medium (0.675 M) eliminate the possibility that the increased permeability is the result of a negative surface potential created by TPB binding, and a carrier mechanism is likely.

TPB and (I) form a precipitate at sufficiently high concentrations, but there is no evidence of precipitate formation in the EPR line shapes at the low concentrations used in these experiments.

DISCUSSION

In the present study, we have shown that it is possible to analyze time-dependent EPR intensities of (I) in the presence of phospholipid vesicles in terms of transmembrane currents of the hydrophobic cation. To carry out this analysis in a quantitative fashion, it is necessary to have values for the binding constant of (I) to the membrane. In the experiments reported here, we find a small apparent asymmetry in the binding to the two surfaces of the vesicle, which, as discussed earlier, may be due to a systematic error in V_{mi}/V_{mo}. In earlier work (Cafiso and Hubbell, 1978), we did not make time-resolved measurements and hence did not obtain K_o, K_i information independently, but assumed $K_i \simeq K_o \equiv K$. In that work K was obtained from equilibrium measurements and hence represented an average binding constant. Because K_i, K_o differ by only 17%, use of the average K caused relatively small errors in calculating equilibrium potentials.

The binding function for (I) to the outer membrane surface, K_oV_{mi}/V_i, was found to be 15.7 ± 0.8. The quantity V_{mi}/V_i can be estimated for the spherical vesicle geometry (Cafiso and Hubbell, 1978) and for reasonable choices of bilayer thickness (40–50 Å), vesicle radius (125–150 Å), and binding region thickness (5–10 Å), we find $100 \geq K_o \geq 50$, which gives a binding energy of ~2–3 kcal/mol. This value is much lower than that for the hydrophobic anion analogue TPB, whose binding constant is on the order of 10^5–10^6 (Ketterer et al., 1971; Andersen and Fuchs, 1975), corresponding to a binding energy of 7–8 kcal/mol.

An important consideration in the interpretation of the experiments presented here is the degree to which the spin label itself perturbs the system. In particular, the flow of (I) across a membrane would be expected to generate a transmembrane electric potential. The magnitude of the charge translocation and the corresponding potential are readily estimated. The total charge per cm^2 flowing through the vesicles during the approach to equilibrium is given by

$$Q = \int_0^\infty i(t)\mathrm{d}t.$$

Using Eq. 15 for $i(t)$,

$$Q = -\frac{ZF}{S_o}\beta\left[\frac{K_oV_{mo}/V_o}{1-\epsilon_o/\epsilon_i}\right]\int_0^\infty \frac{\mathrm{d}A_f}{\mathrm{d}t}\,\mathrm{d}t$$

$$= \frac{ZF}{S_o}\beta\left[\frac{K_oV_{mo}/V_o}{1-\epsilon_o/\epsilon_i}\right][A_f(0) - A_f(\infty)].$$

Thus, the relaxation amplitudes and various constants of the system can be used to estimate the total charge transfer. For the vesicle suspensions used here $Q \simeq 1.0 \times 10^{-9}$ C/cm^2 for $\Delta\psi = 0$ and $Q \simeq 4.4 \times 10^{-8}$ C/cm^2 for $\Delta\psi = -112$ mV. Assuming a membrane specific capacitance of ~1 μF/cm^2, these charge translocations would correspond to potential displacements of 1 mV and 4 mV, respectively, if no other effects were considered. However, even these relatively small potentials will not actually be generated, because the concentration of K^+ used to produce the potential is $>10^4$ times more concentrated than the spin label. Hence, the potential is well buffered against small potential displacements, but even in the absence of any potential buffer capacity, the perturbation due to the spin label is quite small. In the experiments presented in this paper, it should be emphasized that there are only ≈2 phosphonium spin labels per vesicle, and the weak binding guarantees that no significant potential or structural perturbation is produced in the vesicle by the spin label. This statement is supported by the linear binding isotherm (Cafiso and Hubbell, 1978) and the linearity of initial current with concentration of phosphonium (Fig. 3).

In terms of absolute reaction rate theory, the forward translocation rate constant is given by, $k_f = fe^{-\Delta G^{o\ddagger}}/RT$ where f is a universal frequency factor with a value of 6×10^{12} s^{-1} at room temperature and $\Delta G^{o\ddagger}$ is the free energy of the barrier measured with respect to the binding region. With $k_f^o = 7.4 \times 10^{-4}$s^{-1}, $\Delta G^{o\ddagger} = 21$ kcal/mol. A similar calculation for TPB gives a free energy barrier height of 16 kcal in dioleoylphosphatidylcholine membranes (Ketterer et al., 1971). Assuming that $\Delta G^{o\ddagger}$ is essentially all enthalpic, this is close to the barrier height predicted from image force considerations (17 kcal). Bruner (1975) has directly estimated the thermodynamic activation parameters for the hydrophobic anion dipicrylamine (DPA), and concludes that $\Delta G^{o\ddagger}$ for this ion is essentially all enthalpic and is in general agreement with the image force barrier height. As the image force should be similar for TPB, DPA and (I), it is clear that additional factors, amounting to ~4 kcal/mol, contribute to $\Delta G^{o\ddagger}$ for the hydrophobic cation. In addition to membrane dipole potential effects (see McLaughlin, 1977 for an excellent review), the hydration energies of the ester and nitroxide groups on (I) may contribute to the increased barrier height. The relatively low overall permeability of (I) is determined by both a low binding constant to the membrane as well as a small rate constant for translocation caused by the high central barrier.

Pickar and Benz (1978) have studied the transport of tetraphenylphosphonium (TPP) and tetraphenylarsonium (TPA) in planar bilayers. These authors express the ohmic conductivity as $\lambda_o = (Z^2F^2/RT)\beta k_i C$ where C is the (symmetric) concentration of ion, k_i is the forward rate constant at zero potential, and β is a partition coefficient defined as $\beta = N/C$ where N is the number of moles of bound ions per cm^2 of membrane. Eq. 14, written for symmetric concentrations of (I), gives the ohmic conductivity as $\lambda_o = (Z^2F^2)/(RT)\ P\ [I]$, where [I] is the symmetric concentration of the phosphonium. Comparing the Pickar and Benz expression with this, it is clear that $P = \beta k_i$.

Benz and Pickar could not obtain β and k_i separately as is done in the present work, but they do give values of βk_i for various membranes. For dioleoylphosphatidylcholine planar bilayers formed from decane solutions, $\beta k_i = P = 3.4 \times 10^{-9}$ cm/s, which is close to our value of $P = 3.8 \times 10^{-9}$ cm/s for sonicated egg PC vesicles. However, Pickar and Benz find a significant dependence of βk_i on both the membrane forming solvent and the lipid structure, so the close similarity in values may be fortuitous.

The voltage dependencies of the forward rate constant and the rate constant for relaxation to equilibrium are satisfactorily accounted for by Eqs. 8–10 with $n = 0.41$. The parameter n represents the fraction of the total potential drop that occurs from the outer membrane surface to the barrier maximum, and there are several possible explanations for this value. First of all, it is possible that a sharp barrier to ion movement is located in the geometric center of the bilayer. Due to the small radius of curvature of the vesicle, the potential does not vary linearly with distance across the bilayer but varies as $\psi_m(r) = \xi(1/r_o - 1/r)$ where ξ is a constant. When r is the geometric center of the bilayer, the fraction of the transmembrane potential difference that exists from the outer membrane surface to the bilayer center is $r_i/(r_o + r_i) = 0.40$ for $r_i = 100$ Å and $r_o = 150$ Å. This value is quite close to the 0.41 determined experimentally, and a sharp, centrally located barrier is consistent with the results.

However, it should be pointed out that an Eyring rate model using voltage-dependent rate constants of the form of Eqs. 8 and 9 can give mathematically excellent fits to current-voltage curves corresponding to a number of different barrier shapes. For example, Ginsburg and Noble, (1976) show in particular that $n = 0.42$ ($\gamma = 0.42$ in their notation) which may be compatible either with a single Eyring barrier or rectangular, trapezoidal or double rectangular barriers of particular kinds. In fact, $n = 0.44$ fits the image force barrier current-voltage curves quite well.

Values of $n < 0.5$ could also arise if the binding sites for the ions were located within the membrane interior with only a fraction of the total transmembrane potential difference between them. Andersen and Fuchs (1975) invoked this notion of an "effective potential" in explaining field-driven TPB flows in planar bilayers. The effective potential model predicts the binding constants of (I) to the membrane to be significantly potential dependent. However, the values of K_oV_{mi}/V_i derived from the data in Fig. 4 are the same to within ~5%, and we must conclude that (I) binds very closely to the membrane surface such that the total and effective potential difference are the same within experimental error.

The phosphonium ion spin labels such as (I) can, in principle, be used to monitor time-dependent as well as equilibrium potentials across small phospholipid vesicles. A limitation on the time resolution is of course imposed by the rather low membrane conductance of the phosphonium itself. One means of increasing the apparent conductance to phosphonium (I) is to dope the membrane with small quantities of TPB, which apparently acts as a carrier for the ion. The effect of TPB, as shown in Fig. 7, is striking and will clearly give at least one order of magnitude higher time resolution to the method. This approach is potentially useful, because low levels of TPB do not appear to perturb the binding of (I) or the equilibrium concentrations in the presence of a transmembrane potential. The details of this phenomenon are currently under investigation.

APPENDIX A

In this appendix we derive the integrated rate law for the mechanism

$$I_o \overset{K_o}{\rightleftharpoons} I_{mo} \underset{k_r}{\overset{k_f}{\rightleftharpoons}} I_{mi} \overset{K_i}{\rightleftharpoons} I_i$$

The interfacial binding steps are at all times at equilibrium and the transmembrane steps are rate limiting.

Taking the transmembrane step to be elementary, the disappearance of spin label from the external surface is just

$$-\frac{dN_{mo}}{dt} = k_fV_{mo}[I]_{mo} - k_rV_{mi}[I]_{mi} \tag{A1}$$

$$-\frac{dN_{mo}}{dt} = k_fN_{mo} - k_rN_{mi} \tag{A2}$$

The equilibrium binding constants for the outer and inner membrane surfaces are defined as

$$K_o \equiv \frac{[I]_{mo}}{[I]_o} = \frac{N_{mo}}{N_o}\frac{V_o}{V_{mo}} \tag{A3}$$

$$K_i \equiv \frac{[I]_{mi}}{[I]_i} = \frac{N_{mi}}{N_i}\frac{V_i}{V_{mi}} \tag{A4}$$

and mass conservation requires that

$$N_o + N_i + N_{mo} + N_{mi} = N_T, \tag{A5}$$

where N_T is the total number of moles of (I). Eqs. A2–A5 may be combined to obtain an expression for the time rate of change of N_o in terms of N_o as the only variable. The result is

$$-\frac{dN_o}{dt} = \left(N_o\gamma - k_r\frac{K_i}{K_o}\frac{V_{mi}}{V_{mo}}\frac{V_o}{V_i}\frac{N_T}{\epsilon_i}\right), \tag{A6}$$

where

$$\gamma = \left(k_f + k_r \frac{K_i}{K_o}\frac{V_{mi}}{V_{mo}}\frac{V_o}{V_i}\frac{\epsilon_o}{\epsilon_i}\right) \tag{A7}$$

and $\epsilon_o = (1 + K_o V_{mo}/V_o)$; $\epsilon_i = (1 + K_i V_{mi}/V_i)$. At equilibrium, $-dN_o/dt = 0$, and it follows from Eq. A6 that

$$N_o(\infty)\gamma = k_r \frac{K_i}{K_o}\frac{V_{mi}}{V_{mo}}\frac{V_o}{V_i}\frac{N_T}{\epsilon_i}$$

where $N_o(\infty)$ is the equilibrium number of moles in the external solution per liter of vesicle suspension. With this substitution, Eq. A6 becomes

$$-\frac{dN_o}{dt} = \gamma[N_o - N_o(\infty)]. \tag{A8}$$

Direct integration of A8 from time 0 to t gives

$$[N_o - N_o(\infty)] = [N_o(0) - N_o(\infty)]e^{-\gamma t} \tag{A9}$$

From Eqs. A3–A5 and Eq. 9, it may be shown that

$$[N_i(\infty) - N_i] = [N_i(\infty) - N_i(0)]e^{-\gamma t} \tag{A10}$$

Subtracting A10 from A9 and rearranging terms,

$$[N_i + N_o] - [N_i(\infty) + N_o(\infty)] = \{[N_i(0) + N_o(0)] - [N_i(\infty) + N_o(\infty)]\}e^{-\gamma t}. \tag{A11}$$

Recalling Eq. 3 from the text, we see that $A_f = (1/\beta)(N_i + N_o)$, $A_f(\infty) = (1/\beta)[N_i(\infty) + N_o(\infty)]$, and $A_f(0) = 1/\beta\,[N_i(0) + N_o(0)]$. With these results, Eq. A11 can be written in terms of EPR spectral amplitudes as

$$[A_f - A_f(\infty)] = [A_f(0) - A_f(\infty)]e^{-\gamma t} \tag{A12}$$

which is text Eq. 6.

Eq. 10 of the text may be obtained as follows. Using (A3) and (A4) and the voltage dependence of the rate constants (text Eqs. 8 and 9) Eq. A1 can be written as

$$-(dN_{mo})/(dt) = k_f^o e^{-n\phi} V_{mo} K_o [I]_o - k_r^o e^{(1-n)\phi} V_{mi} K_i [I]_i.$$

At equilibrium with $\phi = 0$, $dN_{mo}/dt = 0$ and $[I]_o = [I]_i$. Thus,

$$V_{mo} K_o k_f^o = V_{mi} K_i k_r^o \tag{A13}$$

Including the voltage dependence of the rate constants explicitly and using the identity (A13), Eq. A7 becomes

$$\gamma = k_f^o\left[e^{-n\phi} + \frac{\epsilon_o}{\epsilon_i}\frac{V_o}{V_i}e^{(1-n)\phi}\right].$$

APPENDIX B

In this Appendix, Eq. 11 for the voltage dependence of the phosphonium current density is derived.

The total current density of (I) across the bilayer is defined as

$$i = \frac{ZF}{S_o}[k_f N_{mo} - k_r N_{mi}] = \frac{ZF}{S_o}(k_f V_{mo}[I]_{mo} - k_r V_{mi}[I]_{mi}) \tag{B1}$$

Recalling Eqs. 8 and 9 from the text and (A3), (A4), and (A12) from Appendix A, Eq. B1 may be written as

$$i = \frac{ZF}{S_o} V_{mo} k_f^o K_o \{e^{-n\phi}[I]_o - e^{(1-n)\phi}[I]_i\}. \tag{B2}$$

Defining the permeability P as

$$P \equiv \frac{V_{mo}}{S_o} k_f^o K_o \tag{B3}$$

we have the desired result

$$i = ZFP\,\{e^{-n\phi}[I]_o - e^{(1-n)\phi}[I]_i.$$

APPENDIX C

In this Appendix, Eq. 16, relating the membrane current density to the experimental data, is derived.

The current density, i, is proportional to the flux of (I) across the membrane,

$$i = \frac{ZF}{S_o}(k_f N_{mo} - k_r N_{mi}) = -\frac{ZF}{S_o}\frac{dN_{mo}}{dt}. \tag{C1}$$

Using the definition of the binding constant K_o, it is readily shown that

$$i = -\frac{ZF}{S_o} K_o \frac{V_{mo}}{V_o}\frac{dN_o}{dt}. \tag{C2}$$

Now dN_o/dt must be related to the experimental data, dA_f/dt. To obtain this relationship, we note that the resonance amplitude A_f is related to N_o and N_i by $A_f = (1/\beta)(N_o + N_i)$ where β is defined by Eq. 3 of the text. Thus

$$\frac{dA_f}{dt} = (1/\beta)\frac{d(N_o + N_i)}{dt}. \tag{C3}$$

Now, using mass conservation and the definitions of the binding constants K_o and K_i, it can be shown that

$$\frac{d(N_0 + N_i)}{dt} = \left(1 - \frac{\epsilon_o}{\epsilon_i}\right)\frac{dN_o}{dt}. \tag{C4}$$

From Eqs. C3 and C4 one obtains

$$\frac{dN_o}{dt} = \frac{\beta}{(1 - \epsilon_o/\epsilon_i)}\frac{dA_f}{dt}, \tag{C5}$$

and from C5 and C2 the desired result is obtained:

$$i = -\frac{ZF}{S_o}\beta\left(\frac{K_o V_{mo}/V_o}{1 - \epsilon_o/\epsilon_i}\right)\frac{dA_f}{dt}. \tag{C6}$$

For a convenient approximation good to ~10%, we note that for the experimental conditions used here $(1 - \epsilon_o/\epsilon_i) \approx 1$ and

$$i = -\frac{ZF}{S_o} K_o \frac{V_{mo}}{V_o}\beta\left(\frac{dA_f}{dt}\right). \tag{C7}$$

Eq. C5 may be used to obtain the rate constant k_f^o as follows. At time zero, immediately after mixing (I) with vesicles with $\Delta\psi = 0$, $-dN_o/dt = k_f^o N_o$. Combining this with Eq. C5 and using the definition of β from Eq. 3 of the text, we find

$$k_f^o = -\frac{1}{A_f(0)(1 - \epsilon_o/\epsilon_i)}\left(\frac{dA_f}{dt}\right)_{t=0} \tag{C8}$$

This work was supported by a grant from the National Institutes of Health EY 00729 to Dr. Hubbell; the Jane Coffin Childs Fund for Medical Research, and the Camille and Henry Dreyfus Foundation Award for Young Faculty in Chemistry to Dr. Cafiso.

Received for publication 25 February 1982 and in revised form 1 April 1982.

REFERENCES

Andersen, O., and M. Fuchs. 1975. Potential energy barriers to ion transport within lipid bilayers. *Biophys. J.* 15:795–829.

Andersen, O. S. 1978. Permeability properties of unmodified lipid bilayer membranes. *In* Membrane Transport in Biology. G. Giebisch, D. C. Tosteson, and H. H. Ussing, Editors. Springer-Verlag New York, Inc., New York. 369–446.

Bakeeva, L. E, L. L. Grinius, A. A. Jasaitis, V. V. Kuliene, D. O. Levitsky, E. A. Liberman, I. I. Severina, and V. P. Skulachev. 1970. Conversion of biomembrane-produced energy into electric form. II. Intact mitochondria. *Biochim. Biophys. Acta.* 216:13–21.

Bartlett, G. R. 1959. Phosphorus assay in column chromotography. *J. Biol. Chem.* 234:466–468.

Benz, R., P. Laüger, and K. Janko. 1976. Transport kinetics of hydrophobic ions in lipid bilayer membranes. *Biochim. Biophys. Acta.* 455:701–720.

Bruner, L. J. 1975. The interaction of hydrophobic ions with lipid bilayer membranes. *J. Membr. Biol.* 22:125–141.

Cafiso, D. S., and W. L. Hubbell. 1978. Estimation of transmembrane potentials from phase equilibria of hydrophobic paramagnetic ions. *Biochemistry.* 17:187–195.

Cafiso, D. S., and W. L. Hubbell. 1981. EPR determination of of membrane potentials. *Annu. Rev. Biophys. Bioeng.* 10:217–244.

Castle, J. D., and W. L. Hubbell. 1976. Estimation of membrane surface potential, and charge density from the phase equilibrium of a paramagnetic amphiphile. *Biochemistry.* 15:4818–4831.

Emrich, E. M., W. Junge, and H. T. Witt. 1969 *a*. An artifical indicator for electric phenomena in biological membranes, and interfaces. *Naturwiss.* 56:514–515.

Emrich, E. M., W. Junge, and H. T. Witt. 1969 *b*. Further evidence for an optical response of chloroplast bulk pigments to a light-induced electrical field in photosynthesis. *Z. Naturforsch. Teil. B. Anorg. Chem. Org. Chem. Biochem. Biophys. Biol.* 24 *b*:1144–1146.

Ginsburg, S., and D. Noble. 1976. Use of current-voltage diagrams in locating peak energy barriers in cell membranes. *J. Membr. Biol.* 29:211–229.

Grollman, E. F., G. Lee, F. S. Ambesi-Impiombato, M. F. Meldolisi, S. M. Aloj, H. G. Coon, H. R. Kaback, and L. D. Kohn. 1977. Effects of thyrotropin on the thyroid cell membrane: hyperpolarization induced by hormone-receptor interaction. *Proc. Natl. Acad. Sci. U. S. A.* 74:2352–2356.

Hall, J. E., C.A. Mead, and G. Szabo. 1973. A barrier model for current flow in lipid bilayer membranes. *J. Membr. Biol.* 11:75–97.

Kamo, N., M. Makoto, K. Hongoh, and Y. Kobatake. 1979. Membrane potential of mitrochondria measured with an electrode sensitive to tetraphenylphosphonium, and relationship between proton electrochemical potential, and phosphorylation potential in steady state. *J. Membr. Biol.* 49:105–121.

Ketterer, B., B. Neumcke, and P. Laüger. 1971. Transport mechanism of hydrophobic ions through lipid bilayer membranes. *J. Membr. Biol.* 5:225–245.

McLaughlin, S. 1977. Electrostatic potentials at membrane-solution interfaces. *Curr. Top. Membr. Transp.* 9:71–144.

Macey, R.I., and F.W. Orme. 1980. Permeability of red cells to lipid soluble ions. *In* Membrane Transport in Erthrocytes. Alfred Benzon Symposium. U. V. Lassen, H. H. Ussing, and J. O. Wieth, Editors. Munksgaard, Copenhagen 14:498–518.

Neumcke, B., and P. Laüger. 1969. Nonlinear electrical effects in lipid bilayer membranes. II. Integration of the generalized Nernst-Planck equations. *Biophys. J.* 9:1160–1170.

Pickar, A. D., and R. Benz. 1978. Transport of oppositely charged lipophilic probe ions in lipid bilayer membranes having various structures. *J. Membr. Biol.* 44:353–376.

Shuldiner, S., and H. R. Kaback. 1975. Membrane potential and active transport in membrane vesicles from *Escherichia coli. Biochemistry.* 14:5451.

Singleton, W. S., M. S. Gray, M. L. Brown, and J. L. White. 1965. Chromatographically homogeneous lecithin from egg phospholipids. *J. Am. Oil Chem. Soc.* 42:53–57.

Stark, G. 1980. Negative hydrophobic ions as transport mediators for positive ions. *Biochim. Biophys. Acta.* 600:233–237.

Waggoner, A. S. 1979. Dye indicators of membrane potential. *Annu. Rev. Biophys. Bioeng.* 8:47–68.